Chapter 8

MAGNETOSPHERIC AND HIGH LATITUDE IONOSPHERIC ELECTRODYNAMICS

W.J. Burke, D.A. Hardy, and R.P. Vancour

This chapter deals with the volume of space that is bounded externally by the magnetopause and internally by the plasmapause and the high latitude ionosphere at an altitude of 300 km. The magnetopause separates regions of space dominated by the earth's magnetic field (magnetosphere) and by the shocked solar wind (magnetosheath). Earthward of the plasmapause, dynamics are generally controlled by corotation rather than by solar wind driven convection. The arbitrarily chosen, low altitude boundary in the ionosphere represents a transition below which the effects of the earth's neutral atmosphere are dominant. From the viewpoints of both cause and effect, the chapter is something less than self contained. Without the geomagnetic field (Chapter 4) and the solar wind (Chapter 3), there would be no magnetosphere and no magnetospheric electrodynamics; without solar irradiance (Chapter 2), there would be much less of an ionosphere. Without magnetospheric electrodynamics, there would be no aurora (Chapter 12), no high-latitude currents (Chapter 4), no radiation belts (Chapter 5), and no problems with spacecraft charging (Chapter 7).

The term "electrodynamics" encompasses a complex of processes by which charged particles move about in the magnetosphere-ionosphere system. The nature of the processes varies from region to region within the system. Magnetic merging at the magnetopause and field-aligned potential drops above the auroral ionosphere are examples of localized, electrodynamic processes. They are unified as electrodynamic processes in that they emerge, with appropriate boundary conditions, as solutions of the Vlasov-Maxwell equations. General solutions of the Vlasov-Maxwell equations over the entire magnetosphere-ionosphere system are well beyond present capabilities. Some success, however, has been achieved by considering elements of the system in relative isolation. This provides insight into how system elements evolve in response to external inputs. Since the entire system is electrically coupled, the isolated element approach is self-limiting. As one element evolves it affects processes in other elements of the system. The main goals of this chapter are to describe the various system elements and indicate, in a qualitative sense, how they are electrically coupled.

In dealing with the earth's magnetosphere three things quickly impress the mind. First, there is almost nothing there. Particle densities in the plasma sheet range up to about $1/cm^3$. With present technology, laboratory vacuum systems are able to get down to densities of $10^{10}/cm^3$. Second, the volume of space occupied by the magnetosphere is considerable. Typical magnetospheric dimensions are of the order of 10 R_E (1 R_E = 6.4 × 10^3 km). Third, when concentrated to global scales the effects of magnetospheric processes are impressive. The third point which is illustrated in Figure 8-1 provides a convenient point of departure for this survey of magnetospheric and high-latitude ionospheric processes. The figure exemplifies the spatial distribution of visible radiation observed by means of an optical imaging system on a Defense Meteorological Satellite Program (DMSP) satellite. City lights provide an easily recognized map of the western half of North America. The total energy emitted by auroral forms over the northern tier of Canadian provinces rivals or exceeds the combined ground emissions from the United States and Canada. Auroral emissions are largely due to plasma sheet electrons with energies of a few keV impacting the E layer of the ionosphere. The instantaneous locus of plasma sheet electron precipitation is called the auroral oval. Global imagery from satellites such as DMSP have shown that the auroral oval may be approximated by circular bands surrounding the geomagnetic poles. The centers of the circles are offset by ~3° to the night sides of the magnetic poles. The radii of the circle, the widths of the bands and the intensity of emissions vary with the level of geomagnetic activity. However, at all times the auroral oval exists and acts as a major sink for magnetospheric particles and energy. The particles and energy lost by the magnetosphere due to auroral precipitation ultimately come from the solar wind. Thus, an estimate of global precipitation loss is also an estimate of the efficiency of solar wind/magnetospheric interactions required to maintain the auroras.

During periods of moderate geomagnetic activity the auroral oval can be approximated as a circular band extending from 75° to 65° magnetic latitude. The area of such a band is $10^{17}cm^2$. The mean flux of electrons into the

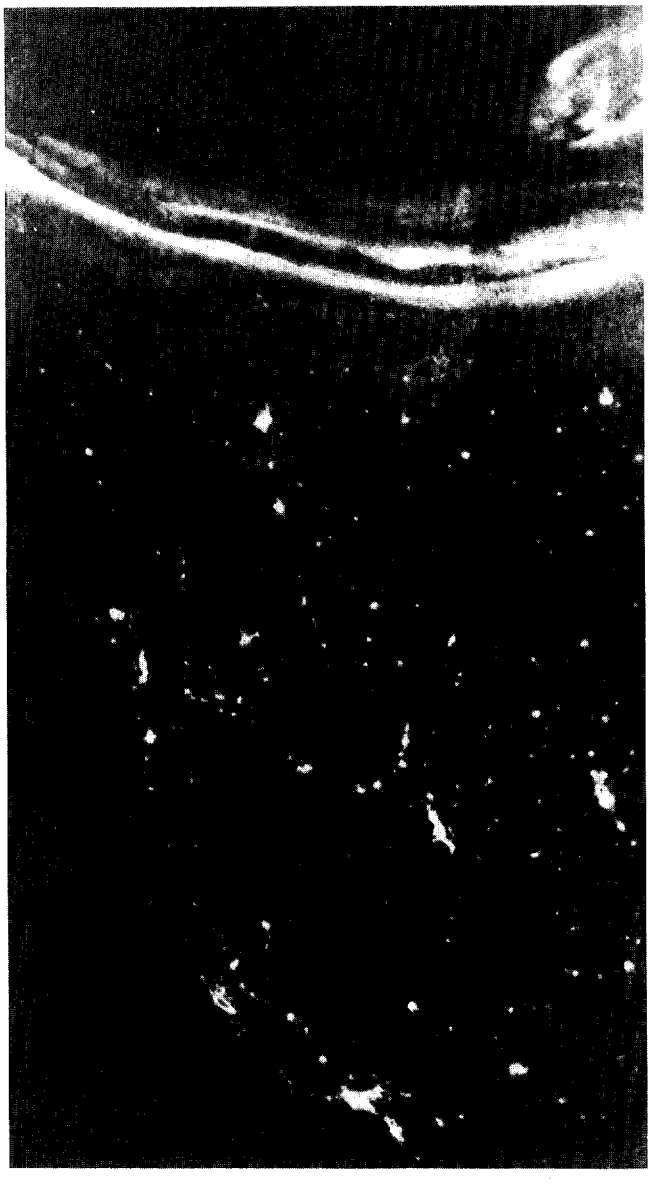

Figure 8-1. DMPS imagery from over western North America.

auroral oval is $\sim 10^9$ cm^{-2}s^{-1}. Thus under steady state conditions the solar wind must supply electrons to the magnetosphere at a rate of 10^{26}/s. The average energy of precipitating electrons is of the order of 1 keV. The energy loss due to electron precipitation alone is $\sim 10^{10}$ W. Similar or larger amounts of solar wind energy must be supplied to account for ionospheric Joule heating and for maintaining the ring current. The central focus of this chapter is to outline the present understanding of how 10^{26} electrons per second and tens of billions of watts are extracted from the solar wind to drive magnetospheric and ionospheric electrodynamic processes.

8.1 MAGNETOSPHERIC BOUNDARY INTERACTIONS

In describing interactions between the solar wind and the earth's magnetosphere two coordinate systems are usefully employed: geocentric solar-ecliptic (GSE) and solar magnetospheric (GSM) coordinates. Both coordinate systems, which are described in detail in Chapter 4, have their origins at the center of the earth with the X axes positive toward the center of the sun; that is, $X_{se} = X_{sm}$. The Z_{se} axis is normal to the ecliptic plane and positive toward the north. The Y_{se} that completes the right hand system is positive toward local dusk. The Z_{sm} axis is coplanar with the earth's magnetic moment vector (**M**) and the X_{sm} axis. It is positive toward ecliptic north. The Y_{sm} axis, which always lies in the SM equatorial plane, completes the right hand coordinate system. For a radially flowing solar wind ($\mathbf{V}_s = -V_s\hat{X}_{se} = -V_s\hat{X}_{sm}$, where $\hat{X}_{se}$ and $\hat{X}_{sm}$ are unit vectors along X_{se} and X_{sm}, respectively) the angle between **M** and Z_{sm} gives the magnetic latitude of the magnetospheric subsolar point. Note that due to 11° offset between **M** and the earths rotational axis and to the 23.5° angle between the equatorial and ecliptic planes the magnetic latitude of the subsolar point is subject to $\pm 34.5°$ combined seasonal and diurnal variations. The GSM is superior to the GSE system for ordering data relevant to interactions between the solar wind and the magnetosphere.

8.1.1 The Magnetopause

The shape of the "steady state" magnetosphere is determined from the force balance equation

$$\nabla \cdot [\underline{\underline{P}} + \underline{\underline{T}}] = 0 \qquad (8.1)$$

where $\underline{\underline{P}}$ and $\underline{\underline{T}}$ are the total pressure and the Maxwell stress tensors, respectively. The total pressure tensor is made up of two parts due to the dynamic and thermal pressures of the solar wind components:

$$\underline{\underline{P}} = 2n_s m_p \mathbf{V}_s \mathbf{V}_s + p_{si} + p_{se} \qquad (8.1)$$

where n_s is the solar wind density, m_p the mass of a proton; p_{si} and p_{se} are the thermal pressures of solar wind ions and electrons, respectively. The factor of 2 accounts for specular reflection of incoming particles. The shape of the magnetopause on the dayside can be calculated by numerical means using a simplified force balance

$$2n_s m_p V_s^2 (-\hat{X}_{se} \cdot \hat{n}_M)^2 = \frac{B_T^2}{2\,\mu_o}, \qquad (8.3)$$

where μ_o is the permitivity of free space, $\hat{n}_M$ is an outward directed unit vector normal to the magnetopause, and $\mathbf{B}_T$

the total magnetic field at the magnetopause. $\mathbf{B}_T$ is a superposition of fields due to the earth's dipole $\mathbf{B}_D$, to the currents flowing on the magnetopause $\mathbf{B}_M$, and to other currents distributed in the magnetosphere. Beyond the magnetopause $\mathbf{B}_M$ exactly cancels the internal fields. To a very good approximation at the subsolar point of the magnetopause

$$|\mathbf{B}_T| = 2|\hat{n}_M \times \mathbf{B}_D|. \tag{8.4}$$

In the magnetic equatorial plane

$$\mathbf{B}_D = \frac{B_o}{L^3}, \tag{8.5}$$

where $B_o = 3 \times 10^4$ nT is the strength of the earth's field at the surface on the magnetic equator and L is the distance from the center of the earth in earth radii (R_E). Substitution of Equations (8.4) and (8.5) into (8.3) gives the distance to the magnetopause near the subsolar point

$$L_M = \left(\frac{B_o^2}{\mu_o n_s m_p V_S^2}\right)^{1/6}. \tag{8.6}$$

For a solar wind density and velocity of 5/cm^3 and 400 km/s, $L_M = 9$. The shape of the dayside magnetopause was calculated by Mead and Beard [1964] and by Olson [1969] using iterative numerical techniques in which the tilt of the dipole was ignored and included, respectively. Figure 8-2 shows a meridional cross section of the magnetosphere calculated with $L_M = 10$ in the Mead and Beard model. The locus of dipole field lines (dashed lines) in comparison with the calculated total field strikingly illustrates the effects of the solar wind on the overall magnetic topology. Magnetic field lines on the dayside are compressed while those on the nightside are elongated. Note that in this model, field lines intersecting the earth at magnetic latitudes greater than 83° are swept back to the nightside by the solar wind. There are a pair of singular points on the magnetopause at separatrices between field lines closing on the day and night sides. These points correspond to the dayside cusps.

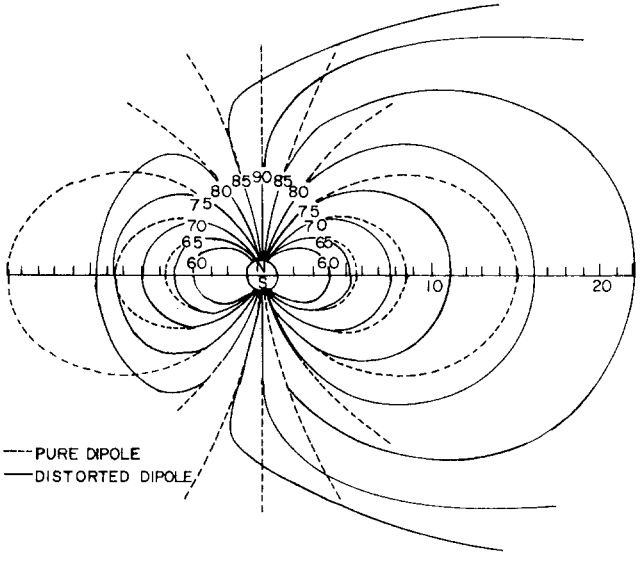

Figure 8-2. Model of earth's magnetic field distorted by the solar wind [Mead and Beard, 1964].

The models just discussed do not describe the nightside of the magnetotail adequately. One reason is apparent from a consideration of Equation (8.2). On the dayside of the magnetosphere, the dynamic pressure of the solar wind dominates over the thermal pressures. On the nightside, with plasma flow almost tangential to the magnetopause ($\mathbf{V}_s \cdot \hat{n}_M \approx 0$), the converse is true. An early model [Johnson, 1950] of the magnetosphere had a tear drop shape with the closing distance determined by the solar wind Mach number. Piddington [1963] suggested that, in flowing past the magnetosphere, the solar wind exerts tangential stresses at the boundary. Such stresses draw the nightside of the magnetosphere into an elongated magnetotail. In the absence of significant plasma within the magnetotail, the tangential force exerted by the solar wind on the magnetosphere is

$$F_T = \frac{B_{MT}^2}{2\mu_o} \pi R_{MT}^2 \tag{8.7}$$

where B_{MT} and R_{MT} are the field strength and radius of the magnetotail, respectively. There are, however, distributed currents in the inner magnetosphere (the ring current) and in the magnetotail (the neutral sheet) currents, whose effects must be included in realistic stress calculations.

8.1.2 Convection

In many cases, the magnetosphere-solar wind interaction is well described by steady state equations such as Equation (8.1). The equilibrium represented by these equations is, however, dynamic rather than static. Only a dynamic situation is consistent with existing high latitude current systems. These currents result from ionospheric convection which is driven by magnetospheric convection [Gold, 1959]. Magnetospheric convection is in turn driven by the solar wind. That is, energy is extracted from the solar wind by the magnetosphere, and at least some of that energy is dissipated in the ionosphere. Two mechanisms for transferring energy to the magnetosphere have been developed over the last two decades: viscous interactions [Axford and Hines, 1961] and magnetic merging [Dungey, 1961]. Both models explain many qualitative features of magnetospheric convection and auroral particle energization. Recent satellite observations suggest that both mechanisms are operative,

but in more complex ways than envisaged by early proponents.

The Axford-Hines model postulates that the magnetosheath plasma exerts a viscous force on a layer of unspecified thickness inside the magnetopause. Magnetic field lines threading this layer are dragged in the antisolar direction and are stretched to great distances in the magnetotail. As elongated flux tubes move out of the viscous interaction layer they snap back to a more dipolar configuration. In the rest frame of the earth this motion of magnetic field lines appears as an electric field, $\mathbf{E} = -\mathbf{V} \times \mathbf{B}$. A magnetospheric equatorial projection of the convection pattern generated in the viscous interaction model is given in Figure 8-3. When mapped to ionospheric altitudes, assuming that

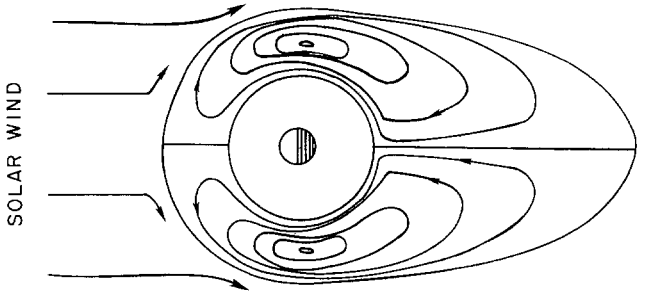

Figure 8-3. Equatorial projection of convection pattern in viscous interaction model.

$\mathbf{E} \cdot \mathbf{B} \approx 0$, the model reproduces the general features of the polar/auroral current system (Chapter 4). Note that plasma trapped on elongated flux tubes is adiabatically heated as the flux tubes convect earthward and shrink in volume.

The second model postulates that the dynamic interaction between the solar wind and the magnetosphere proceeds by means of a magnetic merging process. The simplest features of this phenomenon are illustrated in Figure 8-4.

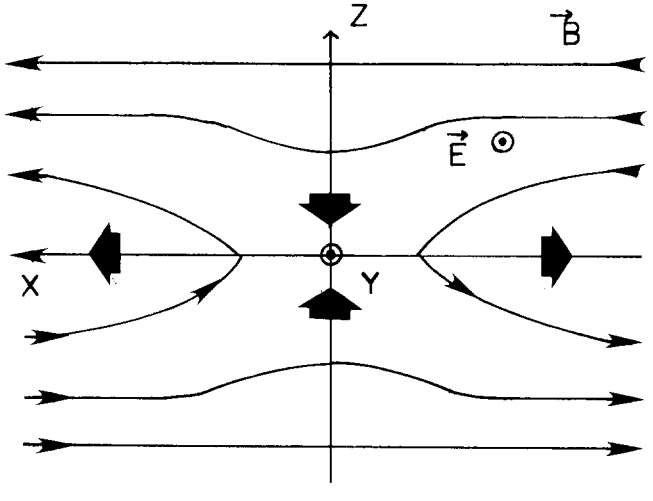

Figure 8-4. Magnetic field geometry and electric field required for magnetic merging.

Consider a magnetic field that at great distances above (below) the X-Y plane points in the + (−) X direction. In the presence of an electric field E_Y, magnetic field lines convect toward the X-Y plane. At the neutral line (X = 0, Z = 0), magnetic field lines from the upper half space merge with field lines of the opposite polarity from the lower half space. To the left (right) of the neutral line, merged magnetic field lines cross the X-Y plane with a + (−) Z component, and $\mathbf{E} \times \mathbf{B}$ convect away from the neutral line in the + (−) direction. Two necessary conditions for magnetic merging are magnetic field of opposite polarity across some plane and an electric field component that is tangent to the plane.

Before considering how magnetic merging might apply to the magnetosphere, it is useful to distinguish between several possible magnetic topologies. It is well known that a weak interplanetary magnetic field (IMF) is carried by the solar wind. Except for a small correction term in the force balance equation, the IMF plays no obvious role in the viscous interaction model. The magnetic merging model assigns important roles to the IMF because this model requires three types of magnetic field lines: (1) IMF lines with both "feet" in the interplanetary medium, (2) closed field lines with both "feet" in the earth, and (3) open field lines with one "foot" on earth and the other in the solar wind. Dungey [1961] pointed out that when the IMF has a southward component, magnetic merging can occur near the subsolar point of the magnetopause. The idea is illustrated in Figure 8-5 which can be viewed either as a snap shot or as

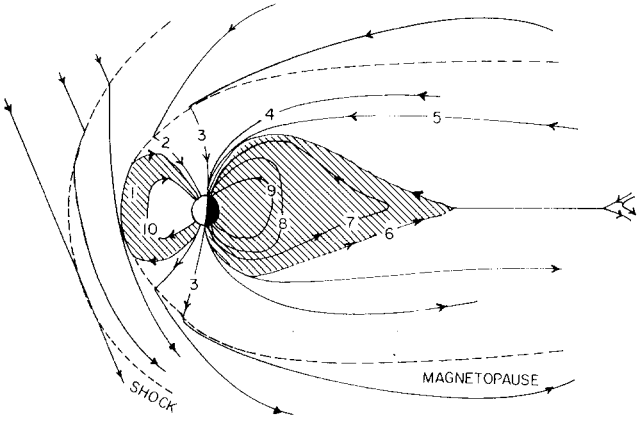

Figure 8-5. Snapshot of magnetic merging between southward IMF and the earth's magnetosphere.

a time history of an individual field line. As southward directed IMF lines are convected up against compressed dipolar field lines, merging occurs at time ①. Because one foot of a newly merged field line is imbedded in the solar wind, the whole field line is dragged in the antisolar ($-X_{sm}$) direction. In an earth-stationary frame of reference the motion of the ionospheric foot of the field line appears to result from a dawn to dusk electric field. Times ② through ⑤ show the various stages of antisunward motion of an open